

# Mechanical Bonding of Aluminum Hybrid Alloy Systems through High-Pressure Torsion

Megumi Kawasaki,\* Seon Ho Jung, Jeong-Min Park, Jongsup Lee, Jae-il Jang, and Jae-Kyung Han

The present study demonstrates an innovative approach of utilizing high-pressure torsion (HPT) processing for the mechanical bonding of dissimilar metals during the microstructural refinement process. This processing approach has been developed recently for introducing unique alloy systems with improving physical and mechanical properties. Accordingly, the present study focuses specifically on the microstructural evolution and development in micro-mechanical responses in the mechanically bonded Al-Mg and Al-Cu hybrid alloy systems when synthesized by HPT processing for very high number of turns up to 60 under 6.0 GPa at room temperature. The microstructural and hardness evaluations confirm the capability of the HPT procedure for the formation of heterostructures with extreme hardness at the disk peripheries and with low hardness at the disk centers in these processed alloy systems. Nanoindentation measurements demonstrate that both hybrid alloy systems exhibit excellent plasticity at the disk edges, where the hardness is the highest. There is a considerable potential for applying the solid-state reaction through the HPT process for the bonding of dissimilar metals as a manufacturing technique and for the development of hybrid alloy systems.

(UFG) materials through the application of severe plastic deformation (SPD), and evaluating the mechanical behavior of UFG materials. Among many of his publications, the comprehensive review articles on processing of UFG metals processed by equal-channel angular pressing<sup>[1]</sup> and by high-pressure torsion (HPT)<sup>[2]</sup> have become significant contributions to our general understanding of SPD processing of UFG materials and those fundamental mechanical properties. Accordingly, it is appropriate that the present study, written to honor Prof. Langdon on his 80th birthday, should be devoted to the examination of microstructural evolution and the mechanical responses of mechanically bonded UFG Al-Mg and Al-Cu alloy systems processed by HPT for high number of turns.

The grain refinement of metallic alloys is achieved in general through the application of thermo-mechanical processing, where

## 1. Introduction

Professor Terence G. Langdon has a long and distinguished research career devoted to describing flow mechanisms of engineering metals and ceramics, processing of ultrafine-grained

different types of treatments are available for separate alloys. However, the achieved grain size in this way is  $\approx 2\text{--}5\ \mu\text{m}$ , and thus, over the last two decades, significant attention was diverted to the application of SPD techniques that are feasible to produce much smaller grain sizes in the submicrometer or nanometer ranges.<sup>[3–6]</sup> Among the available SPD techniques, one of the most effective procedures for grain refinement is the use of HPT, where a bulk metal in the shape of a disk is subjected to a very high compressive pressure and concurrent severe torsional straining.<sup>[2]</sup> A comprehensive history of the HPT processing approach is available elsewhere.<sup>[7]</sup> As SPD processing allows the introduction of significant amounts of point and line defects promoting fast atomic mobility even at ambient temperature within bulk specimens, several SPD techniques including HPT have been proposed as solid-state recycling techniques.<sup>[8]</sup> Moreover, numerous studies are conducted using HPT in the bonding of machining metal chips<sup>[9–12]</sup> and the consolidation of metallic powders.<sup>[13–22]</sup>


The approach of solid-state reaction through HPT has been developed recently for the mechanical bonding of dissimilar bulk metals. In practice, the HPT processing involves a unique sample setup, where two different disk-shaped metallic materials are placed alternately on the lower anvil during the regular processing procedure. This approach is often applied for lightweight metals and alloys to improve their upper limits of mechanical

Prof. M. Kawasaki, J.-K. Han  
School of Mechanical, Industrial and Manufacturing Engineering  
Oregon State University  
Corvallis, OR 97331, USA  
E-mail: megumi.kawasaki@oregonstate.edu

S. H. Jung  
Department of Mechanical Engineering  
Inha University  
Incheon 22212, Republic of Korea

S. H. Jung, Dr. J. Lee  
Metal Forming Technology R&D Group  
Korea Institute of Industrial Technology  
Incheon 21999, Republic of Korea

J.-M. Park, Prof. J.-i. Jang  
Division of Materials Science and Engineering  
Hanyang University  
Seoul 04763, Republic of Korea

 The ORCID identification number(s) for the author(s) of this article can be found under <https://doi.org/10.1002/adem.201900483>.

DOI: 10.1002/adem.201900483

properties, such as strength and ductility, while maintaining constant or further lowering the material density during microstructural refinement and the concurrent bulk-state reaction during processing. Most studies have focused especially on two combinations of Al and Cu<sup>[23–26]</sup> and Al and Mg.<sup>[27–30]</sup>

**Figure 1** shows an overview of the sample cross-sections with the corresponding hardness contour maps for a series of the Al-Mg alloy system processed by the HPT process for 5–20 turns under 6.0 GPa.<sup>[31]</sup> This series of research described the successful bonding of the dissimilar metal disks without any segregation and the nucleation of intermetallic compounds through the diffusion bonding so that the hardness increased significantly at the disk edges where a few different intermetallic phases are created due to severe torsional straining after 10 and 20 turns by HPT.

Accordingly, the present study was initiated to evaluate the microstructural evolution and the micro-mechanical responses in the UFG Al-Mg and Al-Cu alloy systems synthesized by the unique HPT procedure for high torsional revolutions up to 60 turns under 6.0 GPa at room temperature (RT). The evolution in mechanical properties with increasing torsional straining was evaluated for these alloy systems by the novel technique of nano-indentation. The results of this study are expected to expand the capability of the HPT technique from intensive grain refinement to the synthesis of hybrid alloy systems having gradient microstructural features and to the manufacturing procedures of diffusion bonding, welding, and mechanical joining technologies.

## 2. Experimental Section

The experiments for synthesizing an Al-Mg system were conducted using two conventional metals of a commercial purity Al (Al-1050) containing 0.40 wt% Fe and 0.25 wt% Si as major impurities with <0.07 wt% Zn and <0.05 wt% of Cu and Mg as a minor impurities and a commercial ZK60A magnesium alloy containing 4.79 wt% Zn and 0.75 wt% Zr. A plate of Al with a thickness of 1.2 mm was cut into disks with diameters of

≈10 mm by electric discharge machining. The Mg alloy was received as extruded bars having a diameter of 10 mm, and these bars were sliced into disks with thicknesses of ≈1.2 mm. The disks of Al and Mg were then polished to final parallel thicknesses of ≈0.80 mm.

For the synthesis of an Al-Cu system, the consistent commercial purity Al noted earlier and a commercial purity Cu were used in the study. The Cu sample was received as an extruded bar having a diameter of ≈10 mm, and the bar was sliced into disks with thicknesses of ≈1.2 mm. The sliced disks of the Cu were annealed at 673 K for 1 h for homogenization before processing. The disks of Al and Cu were polished to final parallel thicknesses of ≈0.95 and ≈0.83 mm, respectively. As suggested in an earlier report,<sup>[25]</sup> these different thicknesses of the Al and Cu metal disks were selected after a number of careful trials for better mixture of the dissimilar metal phases.

Processing by HPT was conducted with a unique sample setup, which was first reported with a schematic drawing for an Al-Mg system<sup>[27]</sup> with a quasi-constraint HPT facility. In practice, two Al disks and either Mg or Cu disk were alternatively stacked in the order of Al/Mg/Al and Al/Cu/Al without any glue or metal brushing treatment between the disks, and these were placed in the depression on the lower anvil for processing. This processing was conducted under 6.0 GPa at RT for 40 and 60 turns for the Al-Mg system and 20 and 60 turns for the Al-Cu system at a rotational speed of 1 rpm. The processed Al-Mg disks were cut vertically along the diameters into two semicircular disks, and a vertical cross-section on each processed disk was polished to a mirror-like surface and further examined by optical microscopy (OM). The Vickers microhardness values (Hv) were measured at the consistent cross-sections using Mitutoyo HM-200 facility with a load of 100 gf and a dwell time of 10 s. It should be noted that the Vickers microhardness values of the separate Al, Mg, and Cu disks are ≈20, ≈72 and ≈50, respectively.

The microstructural analysis at the disk peripheral regions was conducted by micro X-ray powder diffraction (μXRD) with

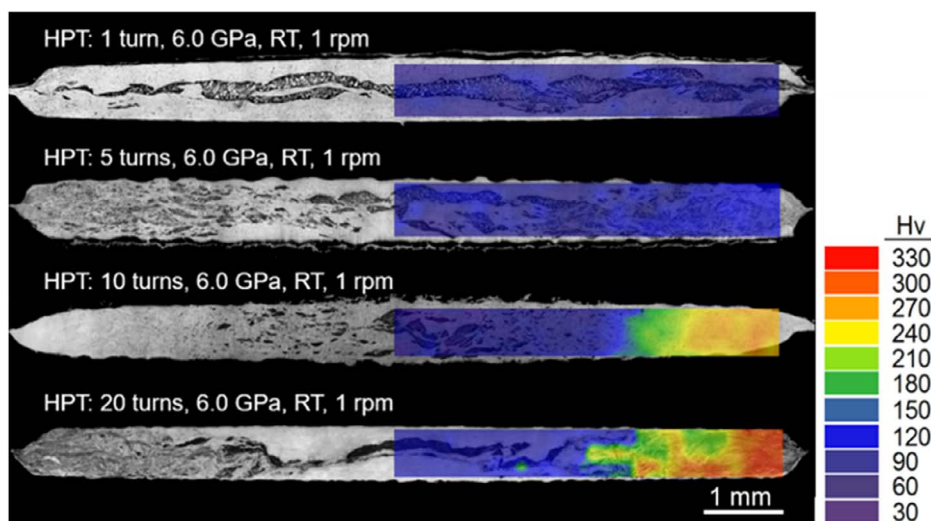


**Figure 1.** Optical micrographs for the disks of the Al-Mg alloy system after HPT for, from the top, 1, 5, 10, and 20 turns, respectively, and the color-coded hardness contour maps are overlapped with the right half of each optical micrograph. Reproduced with permission.<sup>[31]</sup> Copyright 2018, Cambridge University Press.

a Bruker D8-Discover using Cu K $\alpha$  radiation at a scanning speed of 1 min<sup>-1</sup> and a step interval of 0.01° for each examined region of <1.0 mm<sup>2</sup> at 3.5 mm < r < 4.5 mm on a slightly polished disk surface of the Al-Mg system after HPT for 40 and 60 turns, where r is the distance from disk center. Phase identifications and percentages were quantified using XRD data analysis software, Materials Analysis Using Diffraction (MAUD),<sup>[32]</sup> which is based on the Rietveld method.

The micro-mechanical responses were examined at the disk edges in the Al-Mg system after 40 and 60 HPT turns and in the Al-Cu system after 20 and 60 turns using a nanoindentation facility, Nanoindenter-XP (formerly MTS; now Keysight, Santa Rosa, CA) with a three-sided pyramidal Berkovich indenter having a centerline-to-face angle of 65.3°. More than 15 indentations were conducted at the disk edges at each indentation strain rate to provide statistically valid data. All measurements were conducted under a predetermined peak applied load of P<sub>max</sub> = 50 mN at constant indentation strain rates ( $\dot{\epsilon}_i$ ) of 0.0125, 0.025, 0.05, and 0.1 s<sup>-1</sup>, which are equivalent to general strain rates ( $\dot{\epsilon}$ ) of 1.25 × 10<sup>-4</sup>, 2.5 × 10<sup>-4</sup>, 5.0 × 10<sup>-4</sup>, and 1.0 × 10<sup>-3</sup> s<sup>-1</sup> calculated through an empirical relationship.<sup>[33]</sup>

### 3. Results

#### 3.1. Microstructural Evolution and Hardness Development of the Al-Mg System

The overview of the cross-sections and the corresponding hardness distributions are shown in **Figure 2** for the Al-Mg hybrid system after HPT for 40 (upper) and 60 turns (lower). The darker region represents an Mg-rich phase and the brighter region represents the matrix Al phase in the micrographs, and the hardness values were exhibited in the color-coded contour maps with a corresponding color key in right. When comparing the results for up to 20 HPT turns for the Al-Mg system as shown in Figure 1, it was found that increasing numbers of HPT turns expanded the peripheral regions without any visible Mg phases through 40 and

60 turns. It is apparent that these wider peripheral regions recorded significantly high hardness of Hv ≈ 330, while the consistent hardness value was achieved at the small peripheral region of the system after HPT for 20 turns as shown in Figure 1. In practice, the high hardness was observed at the wide peripheries of r ≈ 2.0 mm and >2.0 mm after 40 and 60 HPT turns, respectively, and it was gradually reduced to reach to the lowest hardness value of Hv ≈ 120–150 toward the disk centers at r < 1.5 mm and <0.7 mm for 40 and 60 turns, respectively.

It is reasonable to visualize the hardness evolution with increasing numbers of HPT turns from 1 to 60 for the Al-Mg hybrid system synthesized by the mechanical bonding. **Figure 3** shows the variation of the average Vickers microhardness recorded along the disk diameters at the mid-thickness on the disk cross-sections of the Al-Mg disks after HPT for up to 60 turns. The dotted horizontal lines at Hv ≈ 65<sup>[34]</sup> and ≈110<sup>[35]</sup> are the reference saturation hardness observed for the Al-1050 and ZK60 alloys, respectively, after HPT for 5 turns. It should be noted that the sample after 60 HPT turns shows a visible shift of the disk center in comparison with a typical radial symmetry in hardness distribution of HPT-processed materials.<sup>[36]</sup> It is caused by the inevitable misalignment of the HPT anvils during processing to such a high number of turns. Nevertheless, it is reported that the achieved hardness values with and without misalignment are reasonably consistent except the shifting of the disk center.<sup>[37]</sup>

The hardness plot shows the saturation hardness of Hv ≈ 330 at the disk edge after 20 turns, and it was reasonably maintained constant up to 60 turns. There is a very slow but gradual increase in hardness to Hv ≈ 115 and ≈140 with increasing numbers of turns to 40 and 60, respectively, at the Al-Mg disk centers. The shrinkage of the disk central regions with low hardness as shown in Figure 2 is also visible with increasing HPT turns in the hardness variation plot. It is apparent that the HPT after 10 through 60 turns demonstrated a significant increase in the hardness at the disk edges, and the previous studies on the Al-Mg system processed through 20 HPT turns demonstrated that the high hardness was due mainly to the significant grain refinement

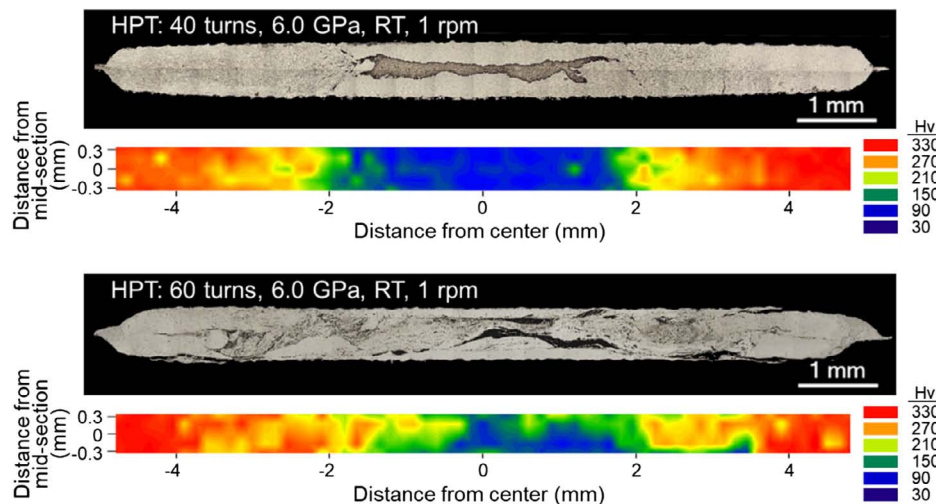


**Figure 2.** Overview of the cross-sections and the corresponding hardness distributions for the Al-Mg system after HPT for 40 (upper) and 60 turns (lower).

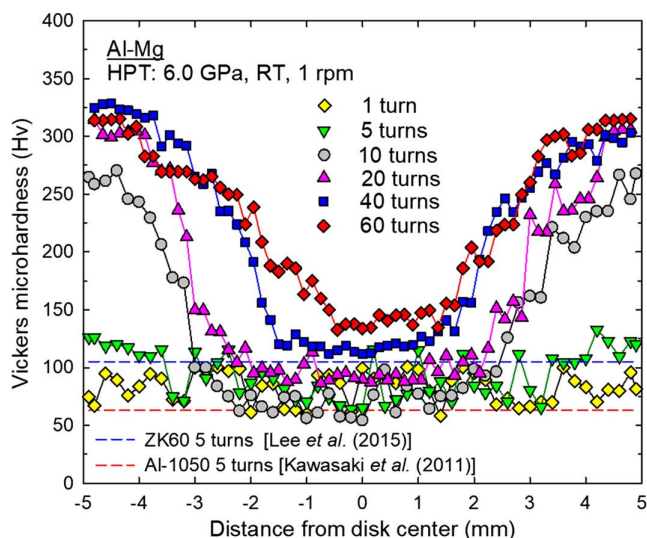


**Figure 3.** The measured hardness values along the disk diameters at the mid-thickness on the cross-sections of the Al-Mg disks after HPT for up to 60 turns.

with a small contribution from the formation of hard intermetallic compounds of  $\text{Al}_3\text{Mg}_2$  and  $\text{Al}_{12}\text{Mg}_{17}$ .<sup>[27–30]</sup>

**Figure 4** shows the XRD line profiles taken by the  $\mu\text{XRD}$  measurements for the disk peripheries of the Al-Mg hybrid disks after HPT for 40 (lower) and 60 turns (upper). It is apparent that consistent strong peaks are detected for a pure *fcc* structure, such as 111, 200, 220, 331, and 222, thereby implying Al, and instead, no clear peaks were found for the intermetallic compounds at both disk edges. The volume fractions of phases estimated by MAUD showed  $\approx 0.01\%$  of both  $\text{Al}_3\text{Mg}_2$  and  $\text{Al}_{12}\text{Mg}_{17}$ , thereby confirming no intermetallic phase in the Al-Mg alloy both after 40 and 60 turns, while there was  $\approx 24\%$  of  $\text{Al}_{12}\text{Mg}_{17}$  in the Al-Mg system processed by HPT for 20 turns.<sup>[30]</sup> As there is almost no significant change in the volume of the disk sample during processing

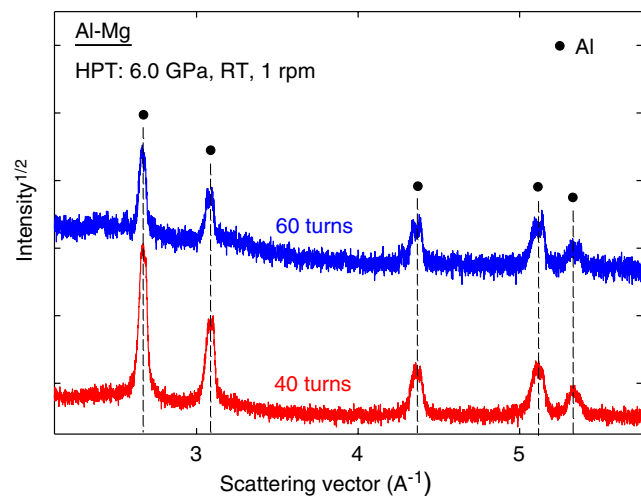


**Figure 4.** XRD line profiles obtained by  $\mu\text{XRD}$  for the disk peripheries of the Al-Mg disks after HPT for 40 (lower) and 60 turns (upper).

by HPT after 5 through 60 turns, it is expected that these intermetallic phases are dissolved into the matrix Al-rich phase at the disk edges of the Al-Mg system during processing for 40 and 60 turns.

The changes in lattice parameter of Al were calculated in comparison with the lattice parameter of pure Al of  $4.049 \text{ \AA}$  by the XRD analysis to provide an estimate of the Mg solubility in the Al matrix<sup>[38]</sup> at the disk edges for 40 and 60 HPT turns. Moreover, the crystallite sizes and the micro-strain were calculated by the Williamson-Hall method using the XRD profiles for the disk edges of the Al-Mg alloy. This method assumes that the full width at half maximum of a Bragg peak is attributed to the contribution of both coherent crystallite size and micro-strain.<sup>[39,40]</sup>

The results are summarized in **Table 1** for the disk edges of the mechanically bonded Al-Mg system by HPT for 40 and 60 turns. Thus, there is a tendency of increasing lattice parameter during HPT, and it is attributed to the increasing dissolution of Mg atoms into the Al lattices with increasing numbers of HPT turns to 40 and 60 turns under a reasonably consistent micro-strain. The results support the increase of Mg concentrations to 6.2 and  $>7.0\%$  in the Al matrix after 40 and 60 HPT turns, respectively, by the dissolutions of Mg atoms existed in the intermetallic phases at the disk edges and in the Mg-rich phase close to the disk centers. Moreover, the microstructure at the disk edges is refined further to a crystallite size of  $\approx 40$  and  $\approx 30 \text{ nm}$  with increasing numbers of turns to 40 and 60, respectively, in comparison with the consistent alloy system after HPT for 20 turns, having a grain size of  $60 \text{ nm}$  measured by a transmission electron microscope.<sup>[30]</sup> The actual grain size is expected to be slightly larger than the crystallite size measured by XRD analysis as described earlier.<sup>[27]</sup> However, this significant grain refinement in the Al matrix is expected to provide a major contribution to such high hardness at the disk edges of the Al-Mg hybrid system after HPT for 40 and 60 turns as shown in Figure 2 and 3. Further investigations are necessary to examine the detailed microstructural changes in the Al-Mg hybrid systems after HPT for such a high number of turns.

### 3.2. Micro-Mechanical Properties of the Al Hybrid Alloy Systems

Considering the significant microstructural evolution involving the disappearance of intermetallic phases, it is reasonable to evaluate the changes in mechanical properties of the Al-Mg system with increasing HPT turns. In practice, the use of the novel technique of nanoindentation is advantageous to acquire mechanical

**Table 1.** Summary of estimated lattice parameter of Al, the concentration of Mg in the Al matrix, the crystallite sizes, and the micro-strain for the disk edges of the Al-Mg alloy processed by HPT for 40 and 60 turns.

	HPT: 40 turns	HPT: 60 turns
Lattice parameter of Al ( $\text{\AA}$ )	4.0773	4.0796
Mg concentration in the Al matrix (at%)	$6.62 \pm 0.3$	$7.14 \pm 0.3$
Coherent crystallite size (nm)	$\approx 41$	$\approx 28$
Micro-strain	0.0143	0.0113



properties from a small sample volume including large microstructural and hardness heterogeneities.<sup>[41]</sup> Thus, the micro-mechanical response was examined using a nanoindentation technique at the disk edges of the Al-Mg hybrid system processed by HPT for 40 and 60 turns.

**Figure 5** shows the representative curves of load versus displacement measured at four equivalent strain rates from  $1.25 \times 10^{-4}$  to  $1.0 \times 10^{-3} \text{ s}^{-1}$  for the edges of the Al-Mg disks after HPT for 40 (upper) and 60 turns (lower). Each curve was obtained as an average of at least 15 measurements, and, in practice, there was no visible broadening between the curves obtained from these separate examinations at each strain rate. Moreover, less broadening, and thus constant mechanical responses, is observed between the curves obtained at four strain rates in the Al-Mg system after HPT for both 40 and 60 turns. From the closer inspection, there are slightly higher displacements after 40 turns than after 60 turns at the maximum load of 50 mN at all strain rates but both samples show positive strain rate dependency of the Al-Mg system synthesized by HPT.

A previous report demonstrated that the Al-Mg disk edge after HPT for 5 turns demonstrated a wide deviation in micro-mechanical response for all 15 nanoindentation measurements at all strain rates, thereby indicating the plastic instability.<sup>[29]</sup> Plastic instability was attributed to the reinforcements of a limited volume of heterogeneously distributed intermetallic phases and the fine Mg-rich phases within the matrix Al-rich phase at the Al-Mg disk edge after 5 HPT turns.<sup>[28]</sup> With increasing numbers of HPT turns to 20, such plastic instability was not observed at the disk edge due to the presence of a large volume of intermetallic phases.<sup>[30]</sup> The present study demonstrated the consistent result with stable mechanical responses at the disk edges of the Al-Mg hybrid system after HPT for 40 and 60 turns. However, from the results, it was found that the Al-Mg hybrid

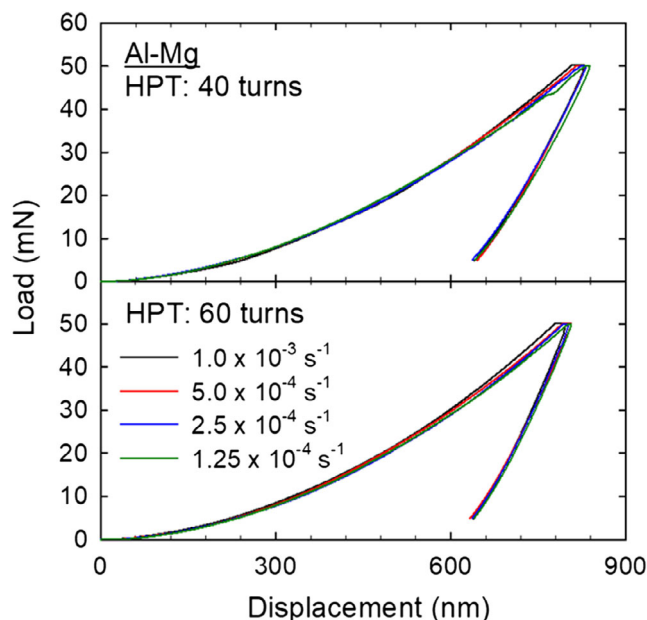


**Figure 5.** Representative curves of load versus displacement measured at four equivalent strain rates from  $1.25 \times 10^{-4}$  to  $1.0 \times 10^{-3} \text{ s}^{-1}$  at the edges of the Al-Mg disks after HPT for 40 (upper) and 60 turns (lower).

system exhibits the stable plasticity due to the presence of single Al-rich phase without any intermetallic phases as shown in Figure 4.

The present study applied the consistent nanoindentation tests on an Al-Cu alloy system synthesized by the HPT processing for 20 and 60 turns. The detailed microstructural evolution during processing was demonstrated in a previous study.<sup>[25]</sup> For a better understanding on the synthesis of the hybrid alloy, it is reasonable to show in **Figure 6a** the overview cross-sections of the Al-Cu disks processed by HPT for 10, 20, 40, and 60 turns<sup>[25]</sup> where the Al-rich phase is shown as a bright phase and the Cu-rich phase is shown in dark-bright color, while these two highly mixed phases are shown in slightly darker gray color in the cross-section micrographs. There is a strong color contrast at the centers of these disks up to 60 turns, where two separate phases of Al and Cu remained without segregation. On the contrary, the disk edges with a grey color represent a mixture of Al and Cu phases, which expanded significantly with increasing numbers of HPT turns. In practice, the disk edge

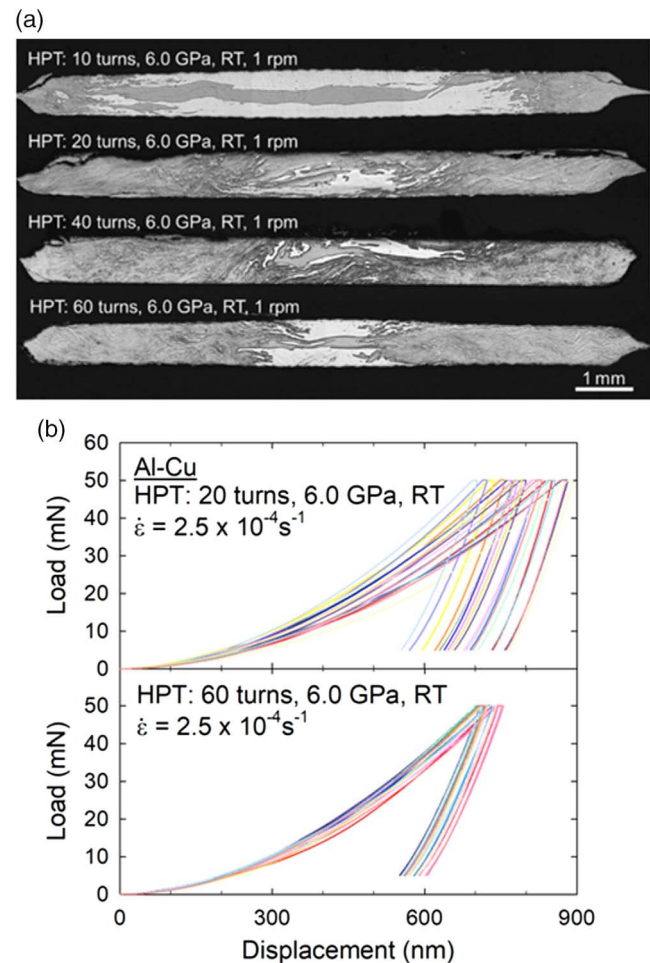


**Figure 6.** a) Overview cross-sections of the Al-Cu disks processed by HPT for 10, 20, 40, and 60 turns. Reproduced with permission.<sup>[25]</sup> Copyright 2018, John Wiley and Sons.; b) Fifteen separate load-displacement curves recorded at an equivalent strain rate of  $2.5 \times 10^{-4} \text{ s}^{-1}$  at the edges of the Al-Cu disks after HPT for 20 (upper) and 60 turns (lower).

at  $r > 3.5$  mm after 10 turns includes very fine Cu phases within the Al matrix. A similar type of microstructure with visible fine Cu phases was observed at the disk edge after 20 turns, while the well-mixed regions of Al and Cu were expanded to  $r > 2.0$  mm. A severe mixture of the Al and Cu phases was further expanded at the disk edges of  $r > 1.0$  mm without any visible Cu phases after HPT for 40–60 turns. Moreover, not only the good mixture and the complete dissolution of Cu, but also the higher amounts of intermetallic phases of  $Al_2Cu$ ,  $AlCu$ , and  $Al_4Cu_9$  were observed at the disk edges for 60 turns, while the amount of intermetallic compounds was limited at the disk edge after 20 turns.<sup>[25]</sup>

The evolution in the microstructural features is expected to influence the mechanical response of the Al-Cu alloy system. Figure 6b shows 15 separate load-displacement curves recorded at an equivalent strain rate of  $2.5 \times 10^{-4} \text{ s}^{-1}$  at the edges of the Al-Cu disks after HPT for 20 (upper) and 60 turns (lower). It is apparent that a series of the curves show a large deviation in micro-mechanical responses for all 15 measurements, thereby indicating the plastic instability at the disk edge after 20 HPT turns. The consistent behavior was recorded for the sample at other three indentation strain rates. However, with increasing numbers of HPT turns to 60, the disk edge of the Al-Cu system tends to show consistent micro-mechanical responses with lower displacement than that after 20 turns, and thus higher hardness, for 15 measurements. Therefore, the mechanically bonded Al hybrid systems involve a gradual phase mixture with a heterogeneous nucleation of intermetallic compounds that tends to demonstrate the plastic instability when torsional strain is not high enough but further straining by increasing numbers of turns leads to consistent mechanical response.

## 4. Discussion

### 4.1. Micro-Mechanical Behavior of Hybrid Systems after HPT

The analysis of a series of load-displacement data sets provides an important mechanical property of plasticity by computing the

strain rate sensitivity ( $m$ ) for the disk edges in the Al-Mg system after HPT for 40 and 60 turns and in the Al-Cu system for 20 and 60 HPT turns, respectively. In the analysis, the value of  $m$  was determined at a given strain ( $\epsilon$ ) and absolute temperature ( $T$ ) by considering Tabor's empirical prediction,<sup>[42]</sup> assuming that the flow stress is equivalent to  $H/3$  in a fully plastic deformation stage at a constant strain rate  $\dot{\epsilon}$ , where  $H$  is the nanoindentation hardness estimated according to the Oliver–Pharr method<sup>[43]</sup>:

$$m = \left( \frac{\partial \ln \sigma_f}{\partial \ln \dot{\epsilon}} \right)_{\epsilon, T} = \left( \frac{\partial \ln (H/3)}{\partial \ln \dot{\epsilon}} \right)_{\epsilon, T} \quad (1)$$

Thus, the slope of the line in a logarithmic plot of  $H/3$  against  $\dot{\epsilon}$  provides an estimated value of  $m$  for each sample and the plots are shown in **Figure 7** for the disk edges of the HPT-induced Al-Mg and Al-Cu alloys. For comparison purposes, the base materials of commercial purity Al and Cu after HPT for 10 turns and their respective  $m$  values are also included in Figure 7b, where these separate materials generally show a reasonable saturation in their hardness responses after  $>5$  HPT turns,<sup>[36]</sup> thereby assuming no significant changes in  $m$  with further increase in HPT turns. A tabulation of strain rate sensitivity ( $m$ ) is available in a previous review for a variety of UFG metals processed by various SPD techniques at specific strain rate ranges at RT measured using different testing methods and conditions.<sup>[41]</sup> It should be noted that although the hardness evolution of the Al-Cu hybrid alloy was reported previously<sup>[25]</sup> and is now shown in this study, the axis of  $H/3$  in the plot provides a positive trend of increasing hardness with increasing numbers of HPT turns.

For the mechanically bonded Al-Mg system by HPT, the  $m$  value was estimated to be 0.018 after 40 turns and it increased to 0.022 after 60 turns. These values are similar to  $m$  value of 0.02 for the base Al after 10 HPT turns as shown in Figure 7b and slightly smaller than  $m \approx 0.03$  obtained by nanoindentation at a mid-diameter of a high-purity Al disk after HPT for 5 turns.<sup>[44]</sup> By contrast, a previous study showed the high  $m$  values of 0.035–0.045 measured by nanoindentation of a ZK60 alloy after HPT for 2 turns.<sup>[45]</sup> However, considering the negative

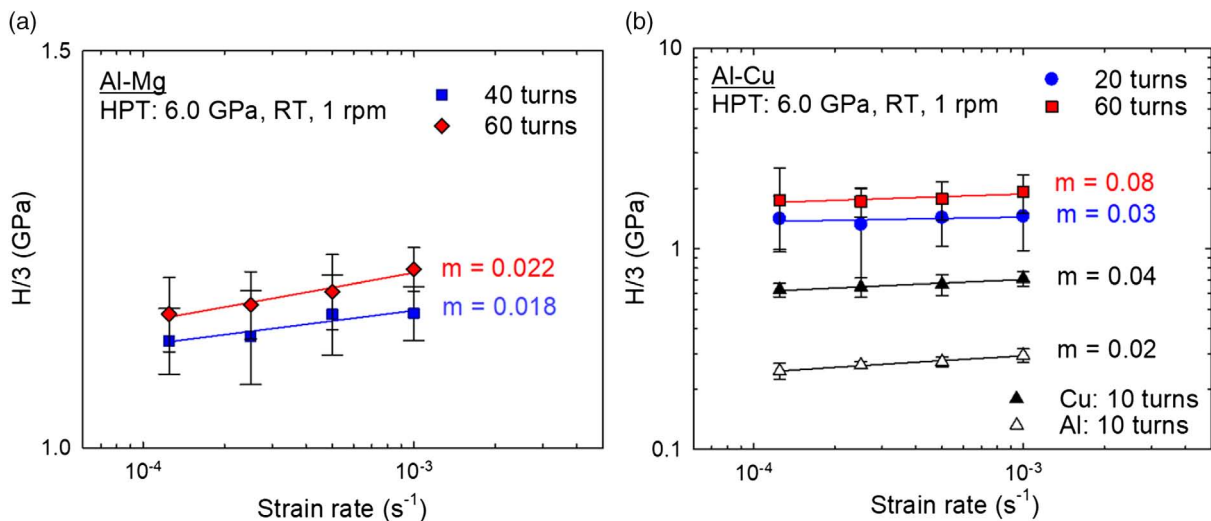


**Figure 7.** Logarithmic plots of  $H/3$  against  $\dot{\epsilon}$  for the disk edges of the HPT-induced (a) Al-Mg alloy and (b) Al-Cu alloy.

strain rate sensitivity of  $m \approx -0.001$  after 20 HPT turns in the HPT-induced Al-Mg alloys,<sup>[30]</sup> the present Al-Mg hybrid alloy demonstrates significant improvement in the strain rate sensitivity, and thus plasticity, with increasing numbers of HPT turns to 40 and 60, respectively. This enhancement in plasticity at the disk edges of the Al-Mg system after 40–60 turns is attributed to the disappearance of the hard intermetallic phases, which pin dislocation motions under severe plastic deformation, while increasing contents of intermetallic compounds as nano-layers embedded in the nanocrystalline matrix led to a typically strong but brittle property relationship in the alloy system at least up to 20 HPT turns.

The strain rate sensitivity was estimated as  $m \approx 0.03$  at the disk edge of the Al-Cu system after HPT for 20 turns in Figure 7b, where the estimation implies the possibility of a lower strain rate sensitivity due to the wider error bars arising from the plastic instability. However, the  $m$  value of the Al-Cu disk after 20 HPT turns is between 0.02 and 0.04, which are the estimated  $m$  values of the base metals of Al and Cu, respectively, after HPT for 10 turns. By contrast, the Al-Cu alloy after 60 HPT turns shows an increased  $m$  value of  $\approx 0.08$ . It is important to note that the microstructure in the disk edge after 20 HPT turns demonstrated a layered nanostructure with layer widths of 20–30 nm, which was thereafter evolved into an equiaxed nanostructure with grain sizes of  $\approx 30$  nm after 60 turns.<sup>[25]</sup> As intermetallic phases in the Al-Cu system also followed the consistent configurational changes from the layers to the equiaxed grains with increasing numbers of HPT turns, it is expected to accelerate the activity of grain boundary sliding, and thus to improve  $m$  value, of the alloy system at RT. Therefore, increasing the number of HPT turns for the hybrid system significantly enhances  $m$  value and thus provides the potential for achieving improved plasticity.

Together with the extreme hardness, the observed excellent plastic responses at the disk edges of these Al hybrid alloys processed by HPT lead to the conclusion that the mechanical bonding and concurrent grain refinement through HPT is an excellent strategy for fabricating lightweight hybrid alloy systems with the possibility of synthesizing a wide variety of new engineering nanomaterials.

#### 4.2. Synthesis of Hybrid Alloys Processed by HPT

The unique sample setup for the conventional HPT processing procedure demonstrates the synthesis of Al hybrid alloys with different levels of gradation in both microstructure and mechanical properties depending on the amount of total straining. In order to visualize a trend of the severe mixture of dissimilar metals by the HPT procedure, it is reasonable to estimate the changes in a boundary radius,  $r_b$ , which is the distance from the disk center dividing the multilayered structure appearing at disk centers from the severe mixture of metal phases appearing at disk edges with increasing numbers of HPT turns in the Al-Mg and Al-Cu systems. The appropriate values of  $r_b$  were estimated using OM images with the sudden hardness increase shown in Figures 1 and 2 for the Al-Mg alloy and in OM images shown in Figure 6a for the Al-Cu alloy.

Figure 8 demonstrates a relationship between  $r_b$  and the estimated equivalent strain and the shear strain for both Al-Mg and

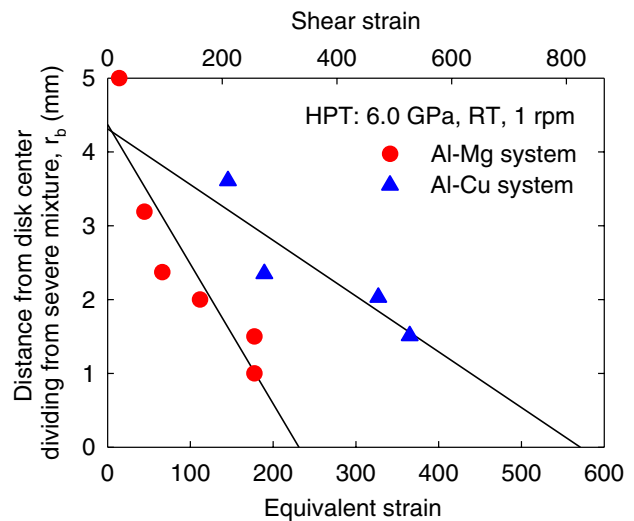


**Figure 8.** A relationship between  $r_b$  and the estimated equivalent strain and the shear strain for both Al-Mg and Al-Cu systems after HPT for 1, 5, 10, 20, 40, and 60 turns and 10, 20, 30, and 40 turns, respectively, under 6.0 GPa.

Al-Cu systems after HPT for 1, 5, 10, 20, 40, and 60 turns and 10, 20, 40 and 60 turns, respectively, under 6.0 GPa. In order to calculate both equivalent strain and shear strain, a disk thickness of  $h \approx 0.7$ – $0.8$  mm was used because the compression stage before commencing the torsional straining provided an outward material flow around the periphery of the disk so that the thickness of the disk under the torsional stage was reasonably constant at  $\approx 0.7$ – $0.8$  mm as shown in Figures 1 and 2 and 6a for both the Al-Mg and Al-Cu systems.

It is apparent from the plot in Figure 8 that there is a linear relationship between  $r_b$  and strain but the rate of change in  $r_b$  depends on the combination of the dissimilar metals. In practice, for a set of metals having wider hardness differences, in the present case for Al-Cu by comparison with Al-Mg, there is a requirement for higher number of HPT turns and thus higher equivalent strain to increase the edge region with a severe mixture of the metal phases. This analysis implies that more than 80 turns and 140 turns are required for the Al-Mg and Al-Cu systems, respectively, to reduce the multilayered central regions to less than 0.5 mm to achieve microstructural homogeneity. There may be additional factors that can accelerate the solid-state reaction and assist the severe mixture, such as the small heat generation during HPT,<sup>[46]</sup> but further experiments are necessary to evaluate the significance of these additional effects.

The present study demonstrated the mechanical bonding of dissimilar bulk metal disks through the application of HPT. As shown in the literature, the first two demonstrations of mechanical bonding required different types of sample setups for HPT processing, where a complete disk consisting of two separate pure Al and Cu semi-circular disks was processed at ambient temperature for up to 100 turns<sup>[23]</sup> and a similar approach was applied with alternately placed two quarter-circles of an Al-6061 alloy and pure Cu at RT for 1 turn.<sup>[24]</sup> Afterward, the HPT processing procedure was further modified for the bonding of separate Al and Mg disks through the stacking of two disks for

up to 20 turns,<sup>[47]</sup> as well as the stacking of three disks, as shown in the present investigations, in order to produce bilayered and multilayered structures, respectively.

The approach of a bulk-state reaction by HPT was studied mainly for the synthesis of hybrid metal systems by utilizing conventional HPT processing through the direct mechanical bonding with significant grain refinement of bulk dissimilar metal disks. In practice, this type of bulk-state reaction by HPT has been demonstrated for Al-Fe,<sup>[31]</sup> Al-Ti,<sup>[31]</sup> Cu-Al,<sup>[26]</sup> Mg-Zn,<sup>[48]</sup> Fe-V,<sup>[49,50]</sup> and V-10Ti-5Cr/Zr-2.5Nb<sup>[51]</sup> systems and a microstructural evaluation has confirmed the capability of the unique HPT processing for rigid bonding with severe mixture of the dissimilar metals and ultimately the formation of unique hybrid nanomaterials in these processed alloy systems. Moreover, this strategy can be successfully applied to a set of alternately stacked 19 Cu and 18 Ta thin foils to form a bulk solid under pressure for up to 150 turns.<sup>[52]</sup> Demonstrating improved both hardness and plasticity in the HPT-induced hybrid alloy systems in comparison with the base metals, this study provides a significant contribution to current developments in diffusion bonding, welding, and mechanical joining technologies.

## 5. Summary and Conclusions

1) The mechanical bonding of engineering metals was successfully demonstrated by using conventional HPT processing under 6.0 GPa at RT through 60 turns for introducing Al-Mg and Al-Cu hybrid alloy systems. 2) The disk edges of the mechanically bonded Al-Mg alloy system by HPT demonstrated exceptional hardness of  $H_v \approx 330$  after 40–60 turns. The  $\mu$ XRD and MAUD analyses estimated the alloy system containing a fully Al-rich phase without any intermetallic phases with crystallite sizes of 40 and 30 nm after 40 and 60 HPT turns, respectively. Moreover, the alloy system demonstrated improved plasticity at the disk edges due to the disappearance of intermetallic phases through such high HPT turns. 3) The Al-Cu system after HPT for 20 turns demonstrated the plastic instability with the strain rate sensitivity of  $m \approx 0.03$ . The mechanical response became stable to show reasonably consistent plastic behavior with the improved strain rate sensitivity of  $\approx 0.08$  after HPT for 60 turns, thereby exhibiting excellent plasticity. 4) Processing by HPT of dissimilar metals demonstrated the feasibility of the introduction of heterostructures in hybrid metals systems leading to variations in mechanical properties. Moreover, the processing procedure enables to develop a wide variety of new hybrid alloy systems and provides a significant contribution to developments in the current bonding and joining manufacturing techniques.

## Acknowledgements

The authors would like to thank Prof. Terence G. Langdon for his long-term support and technical discussion. This study was supported by the National Science Foundation of the United States under grant no. DMR-1810343 (MK & JKH). The work at Hanyang University was supported by the National Research Foundation of Korea (NRF) grants funded by the Ministry of Science and ICT, Nos. 2015R1A5A1037627 and 2017R1A2B4012255 (JMP & Jij).

## Conflict of Interest

The authors declare no conflict of interest.

## Keywords

bulk-state reaction, heterostructure, high-pressure torsion, intermetallic compounds, nanoindentation

Received: April 30, 2019

Revised: June 20, 2019

Published online: August 2, 2019

- [1] R. Z. Valiev, T. G. Langdon, *Prog. Mater. Sci.* **2006**, *51*, 881.
- [2] A. P. Zhilyaev, T. G. Langdon, *Prog. Mater. Sci.* **2008**, *53*, 893.
- [3] R. Z. Valiev, R. K. Islamgaliev, I. V. Alexandrov, *Prog. Mater. Sci.* **2000**, *45*, 103.
- [4] R. Z. Valiev, Y. Estrin, Z. Horita, T. G. Langdon, M. J. Zehetbauer, Y. T. Zhu, *JOM* **2006**, *58*, 33.
- [5] R. Z. Valiev, Y. Estrin, Z. Horita, T. G. Langdon, M. J. Zehetbauer, Y. T. Zhu, *JOM* **2016**, *68*, 1216.
- [6] R. Z. Valiev, Y. Estrin, Z. Horita, T. G. Langdon, M. J. Zehetbauer, Y. T. Zhu, *Mater. Res. Lett.* **2016**, *4*, 1.
- [7] K. Edalati, Z. Horita, *Mater. Sci. Eng. A* **2016**, *652*, 325.
- [8] B. Wan, W. Chen, T. Lu, F. Liu, Z. Jiang, M. Mao, *Resour., Conserv. Recycl.* **2017**, *125*, 37.
- [9] A. P. Zhilyaev, A. A. Gimazov, G. I. Raab, T. G. Langdon, *Mater. Sci. Eng. A* **2008**, *486*, 123.
- [10] K. Edalati, Y. Yokoyama, Z. Horita, *Mater. Trans.* **2010**, *51*, 23.
- [11] M. I. Abd El Aal, E. Y. Yoon, H. S. Kim, *Mater. Sci. Eng. A* **2013**, *560*, 121.
- [12] M. M. Castro, P. H. R. Pereira, A. Isaac, R. B. Figueiredo, T. G. Langdon, *J. Alloys Compd.* **2019**, *780*, 422.
- [13] A. V. Korznikov, I. M. Safarov, D. V. Laptionok, R. Z. Valiev, *Acta Metall. Mater.* **1991**, *39*, 3193.
- [14] V. V. Stolyarov, Y. T. Zhu, T. C. Lowe, R. K. Islamgaliev, R. Z. Valiev, *Mater. Sci. Eng. A* **2000**, *282*, 78.
- [15] X. Sauvage, P. Jessner, F. Vurpillot, R. Pippan, *Scr. Mater.* **2008**, *58*, 1125.
- [16] K. Kaneko, T. Hata, T. Tokunaga, Z. Horita, *Mater. Trans.* **2009**, *50*, 76.
- [17] K. Edalati, Z. Horita, H. Fujiwara, K. Ameyama, *Metall. Mater. Trans. A* **2010**, *41A*, 3308.
- [18] A. Bachmaier, M. Kerber, D. Setman, R. Pippan, *Acta Mater.* **2012**, *60*, 860.
- [19] J. M. Cubero-Sesin, Z. Horita, *Mater. Sci. Eng. A* **2012**, *558*, 462.
- [20] Y. Zhang, S. Sabbaghianrad, H. Yang, T. D. Topping, T. G. Langdon, E. J. Lavernia, J. M. Schoenung, S. R. Nutt, *Metall. Mater. Trans. A* **2015**, *46A*, 5877.
- [21] A. P. Zhilyaev, G. Ringot, Y. Huang, J. M. Cabrera, T. G. Langdon, *Mater. Sci. Eng. A* **2017**, *688*, 498.
- [22] Y. Huang, P. Bazarnik, D. Wan, D. Luo, P. H. R. Pereira, M. Lewandowska, J. Yao, B. E. Hayden, T. G. Langdon, *Acta Mater.* **2019**, *164*, 499.
- [23] K. Oh-ishi, K. Edalati, H. S. Kim, K. Hono, Z. Horita, *Acta Mater.* **2013**, *61*, 3482.
- [24] O. Bouaziz, H. S. Kim, Y. Estrin, *Adv. Eng. Mater.* **2013**, *15*, 336.
- [25] J.-K. Han, D. K. Han, G. Y. Liang, J.-I. Jang, T. G. Langdon, M. Kawasaki, *Adv. Eng. Mater.* **2018**, *20*, 1800642.
- [26] V. N. Danilenko, S. N. Sergeev, J. A. Baimova, G. F. Korznikova, K. S. Nazarov, R. K. Khisamov, A. M. Glezer, R. R. Mulyukov, *Mater. Lett.* **2019**, *236*, 51.



- [27] B. Ahn, A. P. Zhilyaev, H.-J. Lee, M. Kawasaki, T. G. Langdon, *Mater. Sci. Eng. A* **2015**, 635, 109.
- [28] M. Kawasaki, B. Ahn, H.-J. Lee, A. P. Zhilyaev, T. G. Langdon, *J. Mater. Res.* **2016**, 31, 88.
- [29] B. Ahn, H.-J. Lee, I.-C. Choi, M. Kawasaki, J.-I. Jang, T. G. Langdon, *Adv. Eng. Mater.* **2016**, 18, 1001.
- [30] J.-K. Han, H.-J. Lee, J.-I. Jang, M. Kawasaki, T. G. Langdon, *Mater. Sci. Eng. A* **2017**, 684, 318.
- [31] M. Kawasaki, J.-K. Han, D.-H. Lee, J.-I. Jang, T. G. Langdon, *J. Mater. Res.* **2018**, 33, 2700.
- [32] L. Lutterotti, *Nucl. Instrum. Methods Phys. Res. Sect. B* **2010**, 268, 334.
- [33] C. L. Wang, Y. H. Lai, J. C. Huang, T. G. Nieh, *Scr. Mater.* **2010**, 62, 175.
- [34] M. Kawasaki, S. N. Alhajeri, C. Xu, T. G. Langdon, *Mater. Sci. Eng. A* **2011**, 529, 345.
- [35] H.-J. Lee, S. K. Lee, K. H. Jung, G. A. Lee, B. Ahn, M. Kawasaki, T. G. Langdon, *Mater. Sci. Eng. A* **2015**, 630, 90.
- [36] M. Kawasaki, *J. Mater. Sci.* **2014**, 49, 18.
- [37] Y. Huang, M. Kawasaki, T. G. Langdon, *J. Mater. Sci.* **2013**, 48, 4533.
- [38] M. Schoenitz, E. L. Dreizin, *J. Mater. Res.* **2003**, 18, 1827.
- [39] G. K. Williamson, W. H. Hall, *Acta Metall.* **1953**, 1, 22.
- [40] E. J. Mittemeijer, U. Welzel, *Z. Kristallogr. Cryst. Mater.* **2008**, 223, 552.
- [41] M. Kawasaki, B. Ahn, P. Kumar, J.-I. Jang, T. G. Langdon, *Adv. Eng. Mater.* **2017**, 19, 1600578.
- [42] S. Shim, J.-I. Jang, G. M. Pharr, *Acta Mater.* **2008**, 56, 3824.
- [43] W. C. Oliver, G. M. Pharr, *J. Mater. Res.* **1992**, 7, 1564.
- [44] N. Q. Chinh, T. Csanadi, T. Gyori, R. Z. Valiev, B. B. Straumal, M. Kawasaki, T. G. Langdon, *Mater. Sci. Eng. A* **2012**, 543, 117.
- [45] I.-C. Choi, D.-H. Lee, B. Ahn, K. Durst, M. Kawasaki, T. G. Langdon, J.-I. Jang, *Scr. Mater.* **2015**, 94, 44.
- [46] K. Edalati, Y. Hashiguchi, P. H. R. Pereira, Z. Horita, T. G. Langdon, *Mater. Sci. Eng. A* **2018**, 714, 167.
- [47] X. Qiao, X. Li, X. Zhang, Y. Chen, M. Zheng, I. S. Golovin, N. Gao, M. J. Starink, *Mater. Lett.* **2016**, 181, 187.
- [48] D. Hernández-Escobar, Z. U. Raman, H. Yilmazer, M. Kawasaki, C. J. Boehlert, *Philos. Mag.* **2019**, 99, 557.
- [49] S. O. Rogachev, R. V. Sundelev, V. M. Khatkevich, *Mater. Lett.* **2016**, 173, 123.
- [50] S. O. Rogachev, S. A. Nikulin, A. B. Rozhnov, V. M. Khatkevich, T. A. Nechaykina, M. V. Gorshenkov, R. V. Sundelev, *Metall. Mater. Trans. A* **2017**, 48A, 6091.
- [51] S. O. Rogachev, R. V. Sundelev, N. Y. Tabachkova, *Mater. Lett.* **2019**, 234, 220.
- [52] N. Ibrahim, M. Peterlechner, F. Emeis, M. Wegner, S. V. Divinski, G. Wilde, *Mater. Sci. Eng. A* **2017**, 685, 19.